photodissociation of various ligands from porphyrin π cation radicals having the two different types of ground states before these possibilities can be distinguished.

Conclusions

Excitation of the Ru(II) porphyrin π cation radicals, Ru(OEP$^{+\cdot}$)CO(L), with 35-ps 532-nm flashes results in the formation of transient states that decay in <35 ps. There appears to be a correlation between the time constant for the decay and the type of π cation–radical ground state, a <15-ps transient for a $^2A_{1u}$ ground state and an ~25-ps transient for a $^2A_{2u}$ ground state. The kinetic behavior could reflect either decarbonylation followed by geminate recombination or else rapid relaxation via nondissociative states. Analysis of the results indicates that the latter is more likely, but that the former is responsible for at least part of the observed transient behavior cannot be ruled out. The spectra of the transient states suggest that the excited $^2A_{2u}$ ground-state π cation radicals might decay through an $^2A_{1u}$ excited state, while the decay of the excited $^2A_{1u}$ ground-state species with L = Br^- may involve either release and geminate recombination of the Br^- ligand or relaxation of a low-lying CT state with both ligands attached. It is suggested that rapid relaxation to the ground state in all these cases might be enhanced by low-lying (d, π) CT states. In fact, such CT states would tend to make the yield for release of CO from porphyrin π cation radicals lower than from the neutral parent compounds.

Excitation with 355-nm flashes also results in the production of short-lived transients. However, in the cases of the $^2A_{2u}$ ground-state π cation radicals (L = EtOH or py), a long-lived photoproduct is observed, which is ascribed to population of a dissociative state, such as (d_π, d_{z^2}), not accessible with the lower energy 532-nm excitation flashes. The yield is estimated to be <25%. This species is more likely the Ru(III) product obtained upon decarbonylation followed by internal electron transfer than the decarbonylated cation radical itself. This new species appears not to be a degradation product, as a long-lived state is not observed upon photolysis of the cation radical with L = Im, in which the ground state is a mixture of the $^2A_{2u}$ and $^2A_{1u}$. Several reasons for this difference in behavior have been considered, including a more tightly bound CO, more effective low-lying quenching states, and movement of the dissociative state to higher energy in the species having the $^2A_{1u}$ ground state. The relevance of our findings to photodissociation in hemoglobin, myoglobin, and simple metalloporphyrin complexes has been discussed.

Acknowledgment. This work was supported in part by the U. S. National Institutes of Health (AM 17989 and BRSG S07RR07054-17) and the Canadian National Sciences and Engineering Research Council. Funds were also provided to D.H. by a Camille and Henry Dreyfus Foundation Grant for Newly Appointed Faculty in Chemistry. We thank Dr. Maurice Windsor for allowing us to make preliminary measurements with his Nd:glass laser system, and Dr. Martin Gouterman for a careful reading of the manuscript and numerous helpful suggestions.

Registry No. 4a, 80675-21-4; **4b**, 80675-23-6; **4c**, 89463-37-6; **4d**, 87794-43-2; **5**, 55059-73-9; **6**, 38478-17-0; **7**, 89463-38-7.

Spectral Shifts upon Reversible Modifications of CHO Peripheral Substituents in Porphyrin, Chlorin, and Bacteriochlorin. A Phenomenological Explanation for the Red Shift of Protonated Schiff Base

Brian Ward, C. K. Chang,* and Richard Young

Contribution from the Department of Chemistry, Michigan State University, East Lansing, Michigan 48824. *Received October 6, 1983*

Abstract: Previously, we have demonstrated that the formation of a protonated Schiff base metalloporphyrin resulted in a 50-nm red shift of the long wavelength absorption band relative to the unprotonated imine [*J. Am. Chem. Soc.* **1983**, *105*, 634.] A systematic study is now presented on the spectral properties of five formylporphyrin, chlorin, and bacteriochlorin systems upon formation of their protonated Schiff bases. The compounds used in this study were nickel complexes of 4-vinyl-8-formyl, 1,4-diformyl, and 4,8-diformyl derivatives of an alkyl porphyrin; copper 2,6-di-*n*-pentyl-4-vinyl-7-hydroxy-8-acroleinyl-1,3,5,7-tetramethylchlorin; and copper 2,6-di-*n*-pentyl-3,7-dihydroxy-4,8-diacroleinyl-1,3,5,7-tetramethylbacteriochlorin. In addition, pyrrolidine adducts as well as the neutral, but electron deficient condensates of malononitrile and ethyl cyanoacetate were also examined. It was concluded that the unusual red shift of absorption maxima in the visible region and the splitting/broadening of the Soret peak observed in protonated Schiff base porphyrin, chlorin, and bacteriochlorin are attributable to the resonance effect of a strong electron-withdrawing group. Studies of solvent and counterion effects further indicated that the conversion of a carbonyl to a Schiff base peripheral group would subject the spectral and redox properties of chlorin and porphyrin to a greater extent of environmental control. These results suggest that a Schiff base chlorophyll could be an attractive model for the photosynthetic reaction centers.

In many naturally occurring porphyrinoid compounds which contain ketone and/or formyl functional groups, e.g., chlorophylls in photosynthetic apparatii and heme *a* in cytochrome oxidase, it is often observed that the spectral properties of the in vivo and in vitro chromophores do not match.[1,2] This is particularly prevalent for the chlorophylls; for example, the visible absorption band of the chlorophyll reaction center P700 is red shifted relative to chlorophyll *a* (668 nm).[1] Several model studies suggest that P700 is a "special pair" dimer of Chl *a*.[1,3] However, this dimer

(1) (a) Katz, J. J.; Norris, J. R.; Shipman, L. L.; Thurnauer, M. C.; Wasielewski, M. R. *Annu. Rev. Biophys. Bioengineer.* **1978**, *7*, 393–434. (b) Maggiora, G. M. *Int. J. Quantum Chem.* **1979**, *16*, 331–352. (c) Sauer, K. *Annu. Rev. Phys. Chem.* **1979**, *30*, 155–178.

(2) (a) Callahan, P. M.; Babcock, G. T. *Biochemistry* **1983**, *22*, 452–461. (b) Babcock, G. T.; Callahan, P. M. *Ibid.* **1983**, *22*, 2314–2319.

(3) (a) Norris, J. R.; Scheer, H.; Katz, J. J. *Ann. N.Y. Acad. Sci.* **1975**, *244*, 239–259. (b) Fajer, F. J.; Chang, C. K.; Wang, C. B.; Bergkamp, M. A.; Netzel, T. L. *J. Phys. Chem.* **1982**, *86*, 3754–3759. (c) Netzel, T. L.; Bergkamp, M. A.; Chang, C. K. *J. Am. Chem. Soc.* **1982**, *104*, 1952–1957.

0002-7863/84/1506-3943$01.50/0

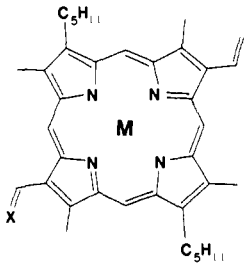

1a X=O M=2H
b X=O M=Ni
c X=NC$_4$H$_9$ M=Ni

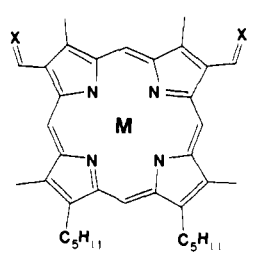

2a X=O M=2H
b X=O M=Ni
c X=NC$_4$H$_9$ M=Ni

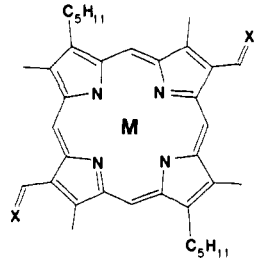

3a X=O M=2H
b X=O M=Ni
c X=NC$_4$H$_9$ M=Ni

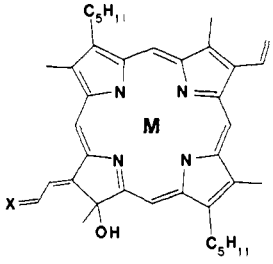

4a X=O M=2H
b X=O M=Cu
c X=NC$_4$H$_9$ M=Cu
d X=N⊕ M=Cu
e X=C(CN)CO$_2$C$_2$H$_5$ M=Cu
f X=C(CN)$_2$ M=Cu
g X=OH,N M=Cu

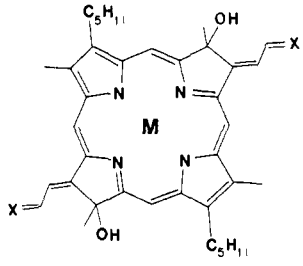

5a X=O M=2H
b X=O M=Cu
c X=NC$_4$H$_9$ M=Cu

Figure 1. Structures and substitution patterns of formylporphyrins **1–3**, acroleinylchlorin **4**, and bacteriochlorin **5**.

model recently has become the topic of considerable dispute, and structurally or physically modified monomeric chlorophylls have been suggested as viable alternatives.[4,5]

Similar to the red shift observed for chlorophylls are the protein influences on the linear polyene retinal, which have been linked to the formation and subsequent protonation of a Schiff base between the retinal –CHO group and a polypeptide lysine group.[6]

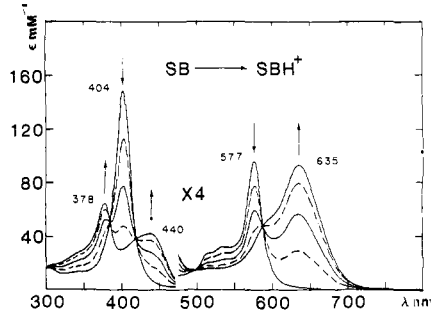

Figure 2. Spectral shifts associated with protonation and deprotonation of Schiff base **1c** in CH_2Cl_2. The arrows indicate the direction of change of the absorption spectrum upon dropwise addition of 70% $HClO_4$-saturated CH_2Cl_2. The dashed (– – –) spectra are those obtained upon addition of Et_3N.

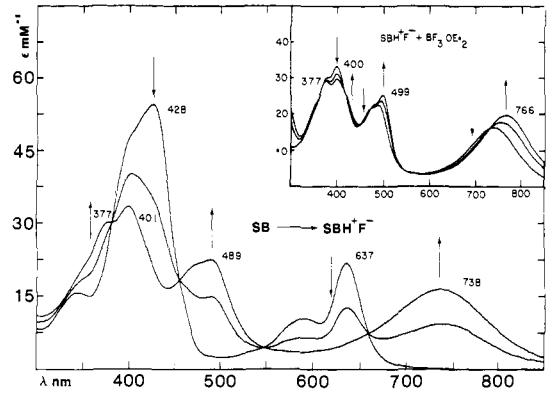

Figure 3. Absorption spectra of Schiff base **4c** protonated with HF vapor in CH_2Cl_2, and conversion of **4c**·HF to **4c**·HBF_4 (inset).

Bearing this in mind, it is interesting to speculate whether porphyrinoid carbonyl moities would react reversibly with nearby amino acid residues in the protein, thereby changing their spectral as well as functional properties. Indeed Wasielewski et al.[4a] have shown that a silyl enol ether of Chl *a* and its analogue 9-desoxo-9-10-dehydrochlorophyll *a* are about 350 mV easier to oxidize than Chl *a* itself. Pearlstein has found that placing a point charge on the periphery of a Chl *a* model compound results in a 4-nm blue shift in the visible absorption band.[4b] In separate experiments, we[5a] and others[5b,c] have shown that substantial red shifts of the visible absorption bands of Schiff base porphyrins and chlorins can occur upon protonation.

In order to better understand the nature of the spectra of protonated Schiff base porphyrin, chlorin, and bacteriochlorin, a systematic study with regard to peripheral substitution and environmental influences is presented here. In the present study, both mono- and diformyl systems with two different substitution symmetries were examined. This detailed phenomenological approach has yielded essential data necessary for a complete understanding of the spectral changes upon protonation. The theoretical aspect of this work is described in the accompanying paper.

Results and Discussion

As shown by the structures in Figure 1, our Schiff base and related derivatives were synthesized from the parent formyl compounds: nickel 2,6-di-*n*-pentyl-4-vinyl-8-formyl-1,3,5,7-tetramethylporphine (**1b**), nickel 1,4-diformyl-6,7-diethyl-2,3,5,8-tetramethylporphine (**2b**), nickel 2,6-di-*n*-pentyl-4,8-diformyl-1,3,5,7-tetramethylporphine (**3b**), copper 2,6-di-*n*-pentyl-4-vinyl-7-hydroxy-8-acroleinyl-1,3,5,7-tetramethylchlorin (**4b**), and copper 2,6-di-*n*-pentyl-3,7-dihydroxy-4,8-diacroleinyl-1,3,5,7-tetramethylbacteriochlorin (**5b**). With the three porphyrins, nickel was inserted because the resultant complexes would be diamagnetic and acid stable and do not readily bind axial ligands. With the chlorin and bacteriochlorin, nickel insertion was more difficult and required prolonged heating which may be

(4) (a) Wasielewski, M. R.; Norris, J. R.; Shipman, L.; Lin, C.-P.; Svec, W. A. *Proc. Natl. Acad. Sci. U.S.A.* **1981**, *78*, 2957–2961. (b) Davis, R. C.; Ditson, S. L.; Fentiman, A. F.; Pearlstein, R. M. *J. Am. Chem. Soc.* **1981**, *103*, 6823–6826. (c) O'Malley, P. J.; Babcock, G. T. *Proc. Natl. Acad. Sci. U.S.A.* **1984**, *81*, 1098–1111.

(5) (a) Ward, B.; Callahan, P. M.; Young, R.; Babcock, G. T.; Chang, C. K. *J. Am. Chem. Soc.* **1983**, *105*, 634–636. (b) Pearlstein, R. M.; Ditson, S. L.; Davis, R. C.; Tentiman, A. F. *Biophys. J.* **1982**, *37*, 112a. (c) Maggiora, L. L.; Maggiora, G. M. *Photochem. Photobiol.*, in press.

(6) (a) Lewis, A.; Marcus, M. A.; Ehenberg, B.; Crespi, H. *Proc. Natl. Acad. Sci. U.S.A.* **1978**, *75*, 4642–4646. (b) Motto, M. G.; Sheves, M.; Tsujimoto, K., Balogh-Nair, V.; Nakanishi, K. *J. Am. Chem. Soc.* **1980**, *102*, 7947–7949.

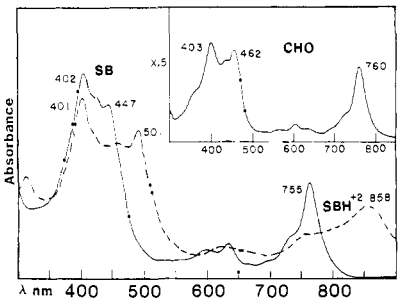

Figure 4. Absorption spectgra of bacteriochlorin **5b** (inset), **5c** (—), and **5c**·$(CF_3COOH)_2$ (---) in THF.

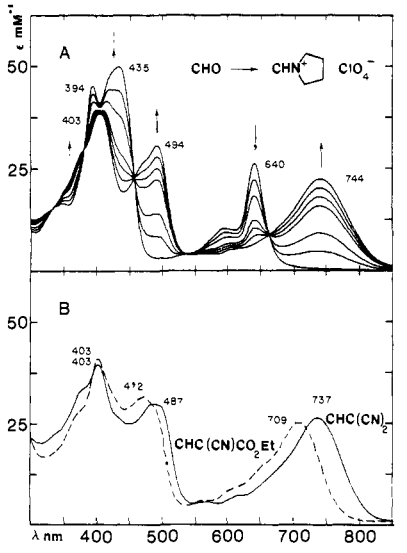

Figure 5. (A) Reaction of aldehyde **4b** with pyrrolidine hydroperchlorate in THF. Total elapsed time = ~1 h. (B) Absorption spectra of ethyl cyanoacetate adduct **4e** (---) and malononitrile adduct **4f** (—) in THF.

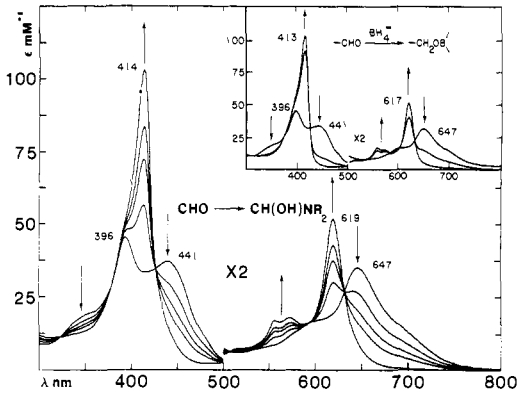

Figure 6. Absorption spectra monitoring the reaction of aldehyde **4b** with excess pyrrolidine in CH_2Cl_2 ($R_2 = C_4H_8$). Reduction of aldehyde **4b** with tetrabutylammonium borohydride in CH_2Cl_2 (inset).

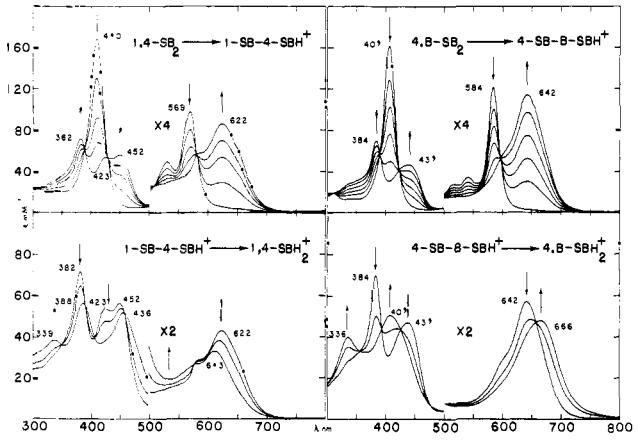

Figure 7. Perchloric acid titrations (70% $HClO_4$ in CH_2Cl_2) of di-Schiff bases **2c** and **3c**. Upper left and right are the first-step protonation of **2c** and **3c**, respectively. Lower left and right are the second protonation step spectra.

detrimental to the integrity of the macrocycle, therefore copper was chosen. The reason that the "photoproto"-type chlorin and bacteriochlorin were used is because of their availability and the fact that the acroleinyl moiety places the CHO group remote enough from the ring to allow facile reaction with a variety of aldehyde-specific reagents; this was not possible for the β-substituted formyl metalloporphyrins owing to steric congestion about the -CHO.

Figure 2 shows the spectral changes associated with protonation and deprotonation of Schiff base **1c** in CH_2Cl_2. The arrows indicate the spectral shifts observed upon addition of 70% perchloric acid-saturated CH_2Cl_2 to **1c**. The dashed spectra are those obtained after bubbling triethylamine-saturated air through the solution. Similarly, Figure 3 shows the spectral shifts observed upon addition of HF vapor to Schiff base **4c** in CH_2Cl_2. Figure 4 contains the spectra of copper bacteriochlorin **5b**, **5c**, and **5c**·CF_3COOH in THF. As shown in Figures 2–4, for all three macrocycles protonation results in relatively large red shifts in the visible absorption maxima with the Soret region becoming split or broadened. The spectral shifts observed upon Schiff base protonation are expected to be present also during iminium salt formation. Indeed, comparison of the spectrum of **4c**·HF (Figure 3) with that of the pyrrolidinium perchlorate (Figure 5a) reveals that this is qualitatively true. Attempts to prepare the pyrrolidinium salt of formylporphyrins (**1b**, **2b**, or **3b**) were not successful.

The dramatic spectral changes associated with Schiff base protonation or iminium salt formation could be due to either delocalization of the positive charge onto the ring or localization of the electropositive hole on the periphery resulting in an electron-deficient group in conjugation with the ring. In order to differentiate between these two possibilities, the electron withdrawing but coulombically neutral ethyl cyanoacetate and malononitrile adducts, e.g., **4e** and **4f**, and other carbonyl derivatives were studied. As shown in Figure 5, the fact that the spectral characteristics of **4e** and **4f** are very similar to those for **4c**·H^+ or **4d** almost immediately rules out the charge-delocalization model. Substitution of an ester for a nitrile moiety, as in **4e** and **4f**, results in a less-electron-withdrawing substituent, and consequently a smaller degree of red shift (**4e** 1520 cm^{-1} vs. **4f** 2060 cm^{-1} shifted from **4b** in THF) as well as less splitting in the Soret region ($\Delta\nu_{4e}$ 3630 cm^{-1} vs. $\Delta\nu_{4f}$ 4280 cm^{-1}). Likewise, spectral perturbation can be brought about by "saturating" the carbonyl group. Figure 6 shows the spectral changes associated with addition of pyrrolidine to **4b** in CH_2Cl_2. The resultant spectrum is essentially identical with that observed after addition of tetrabutylammonium borohydride to **4b** in CH_2Cl_2 (Figure 6 inset). Acidification of the borohydride-treated compound resulted in quantitative conversion to a copper porphyrin.[8,9] Acidification of the pyrrolidine adduct converted it to the pyrrolidinium salt. On the basis of these observations a hemiaminal[10] structure is proposed as the pyrrolidine adduct **4g**. Thus, irreversible reduction or reversible hemiaminal formation produces a blue shift of the visible band by approximately 700 cm^{-1} along with the Soret region coalescing to a single sharp peak. Similarly as observed for all our Schiff bases, replacing O with a less electronegative N during

(7) Fuhrhop, J.-H.; Smith, K. M. In "Porphyrins and Metalloporphyrins"; Smith, K. M., Ed.; Elsevier: Amsterdam, 1975; p 798.
(8) DiNello, R. K.; Chang, C. K. In "The Porphyrins"; Dolphin, D., Ed.; Academic Press: New York, 1978; Vol. I. p 305.
(9) (a) Chang, C. K.; Hatada, M. H.; Tulinsky, A. *J. Chem. Soc., Perkin. Trans. 2* **1983**, 371–378. (b) Chang, C. K., unpublished work. (c) Petke, J. D.; Maggiora, G. M. *J. Am. Chem. Soc.* **1984**, *106*, 3129.
(10) March, J. In "Advanced Organic Chemistry: Reactions, Mechanisms and Structure"; McGraw-Hill: New York, 1968; p 667.

Table I. UV–Visible Spectral Data for Protonated Schiff Base **1c**·HX as a Function of Counterion and Solvent

X^-	solvent	$\Delta\nu_{CHO}$, cm^{-1}	λ_{max}, nm (ϵ, mM^{-1} cm^{-1})			$\epsilon_{380}/\epsilon_{440}$
$F^-(HF^-_2)$	CH_2Cl_2	1205	634 (22)	438 (42)	379 (64)	1.53
Cl^-	CH_2Cl_2	849	620 (21)	432 (48)	377 (52)	1.10
Br^-	CH_2Cl_2	1003	626 (22)	435 (46)	378 (55)	1.18
I^-	CH_2Cl_2	1230	635 (25)	438 (45)	382 (68)	1.55
ClO_4^-	CH_2Cl_2	1230	635 (23)	440 (42)	378 (65)	1.52
$F^- + BF_3$	CH_2Cl_2	1205	634 (22)	438 (42)	379 (64)	1.53
Cl^-	THF	611	611 (18)	417 (56)	376 (43)	0.77
ClO_4^-	THF	797	618 (24)	428 (59)	376 (51)	0.85
Cl^-	CH_3CN	770	617 (24)	427 (56)	373 (54)	0.96
ClO_4^-	CH_3CN	770	617 (24)	427 (56)	373 (54)	0.96

Table II. UV–Visible Spectral Data for Protonated Schiff Base **4c**·HX as a Function of Counterion and Solvent

X^-	solvent	$\Delta\nu_{CHO}$, cm^{-1}	λ_{max}, nm (ϵ, mM^{-1} cm^{-1})			
F^-	CH_2Cl_2	2080	738 (16)	489 (22)	400 (33)	377[a] (30)
Cl^-	CH_2Cl_2	2080	738 (16)	487 (23)	401 (33)	377[a] (29)
Br^-	CH_2Cl_2	2220	746 (17)	498 (23)	401 (34)	378[a] (30)
I^-	CH_2Cl_2	2570	766 (20)	499 (25)	400 (30)	377 (30)
ClO_4^-	CH_2Cl_2	2570	766 (20)	499 (25)	400 (31)	377 (30)
$F^- + BF_3$	CH_2Cl_2	2570	766 (20)	499 (25)	400 (29)	377 (30)
Cl^-	THF	1420	704 (19)	478 (29)	403 (40)	
ClO_4^-	THF	2020	735 (20)	490 (30)	404 (37)	
Cl^-	CH_3CN	1960	732 (23)	487 (32)	399 (38)	375[a] (31)
ClO_4^-	CH_3CN	1980	733 (23)	487 (33)	399 (38)	375[a] (30)

[a] Shoulder.

Table III. UV–Visible Spectral Data of **4d**·X^- as a Function of Counterion and Solvent Composition

X^-	solvent	$\Delta\nu_{CHO}$, cm^{-1}	λ_{max}, nm (ϵ, mM^{-1} cm^{-1})			
Cl^-	CH_2Cl_2	2650	771 (23)	500 (29)	402 (33)	380 (30)
Br^-	CH_2Cl_2	2770	778 (24)	502 (28)	402 (32)	378 (29)
ClO_4^-	CH_2Cl_2	3310	812 (25)	507 (28)	402 (27)	375 (29)
Cl^-	THF	2090	739 (20)	491 (27)	400 (42)	
Br^-	THF	2130	741 (22)	492 (29)	402 (39)	
ClO_4^-	THF	2180	744 (24)	494 (30)	403 (38)	
Cl^-	CH_3CN	2040	736 (23)	489 (31)	399 (44)	378[a] (33)
Br^-	CH_3CN	2040	736 (24)	489 (31)	398 (42)	378[a] (33)
ClO_4^-	CH_3CN	2040	736 (24)	489 (33)	399 (40)	378[a] (32)

[a] Shoulder.

Schiff base formation leads to a blue shift of the visible band relative to their parent formyl or acroleinyl compounds.

From a phenomenological perspective, the above data combined with earlier NMR and Raman studies leave little doubt that the unusual spectral properties of protonated Schiff base porphyrinoid derivatives are brought about by the presence of a conjugating electron-deficient substituent on the ring. It would be reasonable to expect that the spectral shifts upon Schiff base protonation should also be dependent on the substitution pattern of the macrocycle.

Figure 7 shows the spectral shifts observed upon addition of 70% $HClO_4$-saturated CH_2Cl_2 to di-Schiff bases **2c** and **3c** in methylene chloride. The two upper sets of spectra are the first protonation step while the lower are the second. The final monoprotonated SB spectra were not obtained directly. They were resolved by incremental subtraction of the free Schiff base spectra from a mixture of the free and monoprotonated SB until the spectrum matched that obtained from incremental subtraction of the diprotonated SB spectrum from a mono- and diprotonated SB mixture. The essential difference between di-Schiff base **2c** and **3c** is that the formyl groups lie on either different or the same molecular axis. As shown in Figure 7, the second protonation step of **2c** results in a 240-cm^{-1} blue shift of the visible band and a red shift of the split Soret. This behavior is exactly reversed with the diametrical (same axis) di-Schiff base **3c** in which the visible band is further red shifted by 560 cm^{-1} and the Soret region blue shifted. Therefore, these results provide experimental evidence that the red shifts observed for Schiff base protonation are partially due to perturbation along one porphyrin axis. If single-axis perturbation were solely responsible for the observed shifts then it would be expected that the second protonation step of **2c** would result in returning the spectrum much more toward the unprotonated Schiff base. Since diprotonated **2c** and diformyl **2b** are both red shifted relative to **2c**, it appears that the red shift of the visible band as well as Soret splitting is also partially attributable to the increased electron-withdrawing capability of $CH{=}NH^+R$ and CHO relative to $CH{=}NR$.

Environmental Effects. If the SBH^+ formation should leave the positive charge localized on the ring peripheral group, the environment of a protonated Schiff base should also modify its electron-withdrawing strength, providing a pathway for spectral tuning. Conceivable mechanisms include ion pairing, solvation, and hydrogen bonding from SBH^+ to an acceptor. In discussing solvent and anion effects on the spectra of SBH^+ and pyrrolidinium salts, we will use the relative difference $\Delta\nu_{CHO}$, where the frequency in wavenumbers of the visible band for **1b** in CH_2Cl_2 and **4b** in THF is taken as a reference point. Quantitative comparison of the spectral maxima for **4c**·HX and **4d**·X^- is avoided here for three reasons: (1) molecular bulk at the imino nitrogen between the two compounds is different leading to different solvation, (2) the proton of SBH^+ may form a H bond to the 7-hydroxyl group, and (3) H bonding may occur between the SBH^+ proton and the

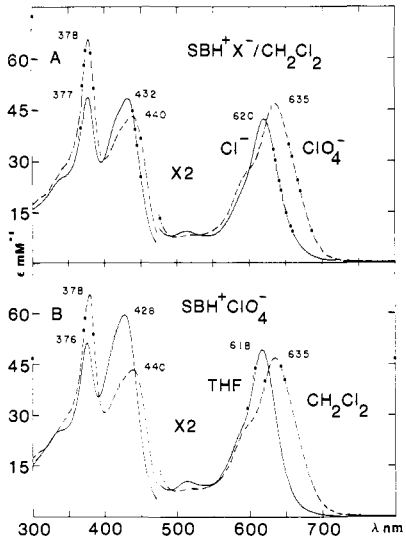

Figure 8. Counterion and solvent dependence of the absorption spectrum for protonated Schiff base **1c**: (A) **1c**·HCl (—) and **1c**·$HClO_4$ (---); (B) **1c**·$HClO_4$ in THF (—) and in CH_2Cl_2 (---).

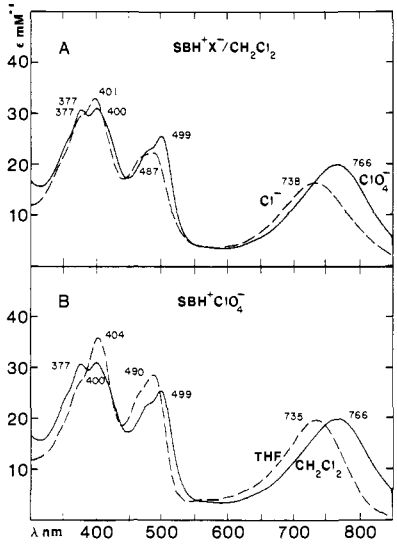

Figure 9. Solvent and counterion dependence of the spectrum for protonated Schiff base **4c**: (A) **4c**·HCl (---) and **4c**·$HClO_4$ (—) in CH_2Cl_2; (B) **4c**·$HClO_4$ in THF (---) and in CH_2Cl_2 (—).

counteranion, resulting in mixed effects.

Figures 8–10 as well as Tables I–III contain the absorption spectral data for SBH^+ **1c**, **4c**, and pyrrolidinium salt **4d** as a function of counteranion and solvent. For porphyrin **1c** in CH_2Cl_2, with the exception of F^-, we observed that the visible absorption maxima vary by 380 cm^{-1} with the larger anions producing larger red shifts. Concomitantly, the lower-energy Soret band red shifts and the Soret intensity ratio ($\epsilon_{380}/\epsilon_{440}$) increases with increased counteranion size. The position of the 380-nm Soret band remains essentially unaltered. This effect is also present in THF (though less pronounced) but absent in acetonitrile. Titration of **1c** with HF in CH_2Cl_2 resulted in a spectrum essentially identical with that of $SBH^+ClO_4^-$ and was not altered upon addition of BF_3·OEt_2, indicating that the pK_a of SB **1c** is less than the equilibrium constant for HF_2^- (K_{eq} = 5–25[11a]). Similarly, the visible absorption maxima are varied by 490 and 660 cm^{-1} in CH_2Cl_2 for **4c**·HX and **4d**·X^-, respectively, with the extent of red shift being again dependent on anion size. In THF, the counteranion effect on **4c**·HX and **4d**·X^- varied $\Delta\nu_{CHO}$ by 600 and 90 cm^{-1}, respectively. In acetonitrile, we observed essentially no counteranion effect for either **4c**·HX or **4d**·X^-. The anion dependence in the Soret region of chlorins **4c**·HX and **4d**·X^- also paralleled that of porphyrin **1c**·HX. There is, however, a difference in the protonation of Schiff

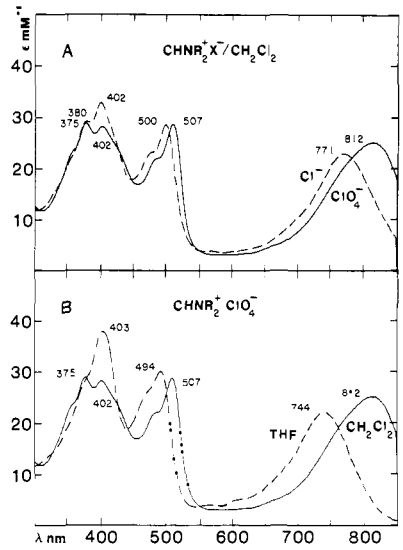

Figure 10. Solvent and counterion dependence of pyrrolidinium salt **4d** (R_2 = C_4H_8): (A) **4d**·Cl^- (---) and **4d**·ClO_4^- (—) in CH_2Cl_2; (B) **4d**·ClO_4^- in THF (---) and in CH_2Cl_2 (—).

base **1c** vs. **4c** with HF. The spectrum of **4c**·HF in CH_2Cl_2 is essentially identical with that of 4c·HCl (Table II), and the spectrum of **4c**·HBF_4 (obtained from addition of BF_3·OEt_2 vapor to **4c**·HF[11b]) is identical with that of 4c·$HClO_4$ (see Figure 3 inset and Table II). This could be the result of two effects: the pK_a of **4c** is higher than the HF_2^- equilibrium constant or, more likely, the presence of the 7-hydroxyl moiety aids in fluoride association with **4c**·HF, thereby lowering the "free" fluoride concentration.[11c]

The anion dependence on the spectral properties of pyrrolidinium salt **4d** is clearly the result of ion pairing; however, the anion dependence of protonated Schiff bases (**1c**·HX and **4c**·HX) cannot be regarded so simply. Compounds **4c**·HX and **4d**·X^- have very similar anion dependencies in CH_2Cl_2 yet different dependencies in THF. In solvents of relatively low dielectric constants, we expect that the smaller anions are closely associated with the positive charge, producing smaller $\Delta\nu_{CHO}$ with decreasing anion size. For **4d**·X^- this accounts for only 90 cm^{-1} in THF while for **4c**·HX there is a 600-cm^{-1} difference. This phenomenon may be the result of Cl^- H bonded to SBH^+. The diminished anion effect of **4d**·X^- in THF relative to CH_2Cl_2 is rationalized as arising from positive charge solvation.

Since using perchlroate as the counteranion for protonated **1c** and **4c** as well as **4d** produced the largest red shifts, we assume that in the three solvents used, ion pairing with perchlorate is minimal. In THF and acetonitrile, we expect that a positive charge will be much more solvated than that in CH_2Cl_2. For pyrrolidinium perchlorate **4d** this produces a $\Delta\Delta\nu_{CHO}$ of 1130 cm^{-1} (CH_2Cl_2 vs. THF) and 1270 cm^{-1} (CH_2Cl_2 vs. CH_3CN); for **4c**·$HClO_4$, the solvent dependence is 550 cm^{-1} (CH_2Cl_2 vs. THF) and 590 cm^{-1} (CH_2Cl_2 vs. CH_3CN) and for **1c**·$HClO_4$, 430 cm^{-1} (CH_2Cl_2 vs. THF) and 460 cm^{-1} (CH_2Cl_2 vs. CH_3CN). However, again we cannot ascribe a single dominating effect to the shifts observed for SBH^+. We would expect that hydrogen bonding from a protonated Schiff base would result in a blue shift relative to a non-H-bonded SBH^+. Since the pyrrolidinium perchlorate spectral data suggest large contributions from solvation on the extent of visible band red shifting, comparison of **4c**·$HClO_4$ to **4d**·ClO_4^- spectral data in H-bond accepting solvents (i.e., THF) vs. nonaccepting solvents (i.e., CH_2Cl_2) would lead to no useful conclusions.

The presence of a hydroxyl group in chlorin **4** offers a unique opportunity for studying the effect of intramolecular H bonding to CHO or CH=NR. In CH_2Cl_2 we observed that the visible absorption maximum of **4b** is red shifted by 170 cm^{-1} with further splitting of the Soret region relative to THF (Figure 11). This effect can be titrated away with a variety of hydrogen bond acceptors, i.e., amines and ethers. The inset in Figure 11 shows such a titration with pyridine. We observed no solvent dependence

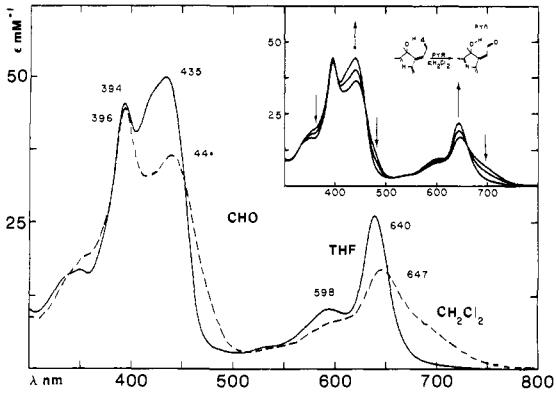

Figure 11. Absorption spectrum of **4b** in THF (—) and in CH_2Cl_2 (---). Inset shows the spectral shifts observed upon dropwise addition of pyridine to **4b** in CH_2Cl_2.

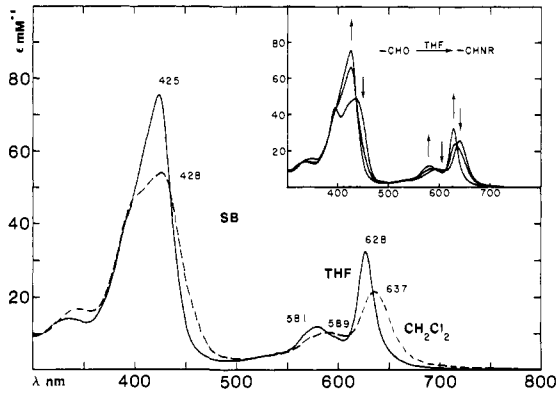

Figure 12. Absorption spectra of *n*-butyl Schiff base **4c** in THF (—) and CH_2Cl_2 (---). Conversion of **4b** to Schiff base **4c** in THF with excess *n*-butylamine and catalytic amounts of HCl (inset).

on the spectrum of **1b**. From the previous discussion, the visible absorption band position and Soret splitting are a function of the electron-withdrawing strength of the peripheral substituent. Intuitively it is expected that a H-bonded –CHO is more electron withdrawing than a "free" CHO. We believe the spectral differences of **4b** in CH_2Cl_2 vs. THF are principally due to intramolecular hydrogen bonding between –CHO and the 7-OH group in CH_2Cl_2, whereas in THF, the OH primarily interacts with solvent. Similar red shifting has been observed for copper porphyrin *a* on addition of H-bond donors in CH_2Cl_2.[2b] By the same arguments for aldehyde **4b**, the Schiff base **4c** also forms an intramolecular hydrogen bond. In the absorption spectrum (Figure 12), this is reflected as a 230-cm^{-1} red shift to the visible band and an overlapped splitting (broadening) of the Soret peak.

Besides solvent and anion effects demonstrating the variability of the spectral shifts associated with Schiff base protonation, evidence for separation of the in-plane polarized transition dipoles is also provided. The effect of solvent and anion on the Soret region in general shows that the position of the higher energy Soret component remains essentially invariant while the lower energy component parrallels the shifts observed by the visible region absorbance maximum (see Figures 8–10 and Tables I–III). Since the lower-energy Soret component is sensitive to ion pairing, solvation, and hydrogen bonding, it seems logical to conclude that the lower-energy Soret band is predominantly the in-plane polarized transition dipole along the protonated Schiff base axis, while the invariability of the higher-energy Soret band suggests it is the other polarization transition dipole. Confirmations of this assignment are presented in the accompanying paper.

Redox Potentials. Electrochemical redox potentials of porphyrinoid compounds often give useful information concerning the orbital energies of the system since, to a first approximation, the redox span of the monocation to monoanion radical formation corresponds to the HOMO-LUMO energy gap.[12] Unfortunately,

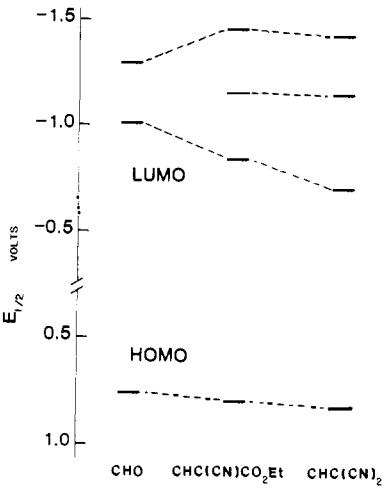

Figure 13. Half-wave redox potentials of aldehyde **4b**, ethyl cyanoacetate adduct **4e**, and malononitrile adduct **4f**, measured in THF vs. SCE.

cyclic voltammograms for **4c**, **4c**·HX, or **4d** gave only ill-defined redox waves. Therefore, the aldehyde **4b**, ethyl cyanoacetate **4e**, and malononitrile **4f** adducts were investigated as models. The $E_{1/2}$ of these compounds in THF are reproduced in Figure 13. There were apparently coupled irreversible waves at −1160 and 40 mV for **4e** and at −1150 and 130 mV for 4f, which were absent in **4b** and are probably due to redox reactions occurring at the ring periphery.

While it may be difficult to asertain to what extent Coulombic forces will perturb the redox potentials of SBH^+, the model studies indicate it seems certain that SBH^+ will be easier to reduce but somewhat harder to oxidize than the parent aldehyde (Figure 13). As is the case with monoformyl vs. diformylporphyrins,[9a] the effect of increasing the electron-withdrawing power of the substituents serves to decrease the HOMO-LUMO gap, indicating the presence of strong resonance effect. Also similar to formylporphyrins, the electron-withdrawing substituents seem to mostly affect the energy of the LUMO. This has been interpreted as evidence that the substituent high-lying π^* mixes with the macrocycle π^* orbital.[9c] Therefore, protonation of Schiff bases further splits the excited states degeneracy and lowers the π^* orbital energies, but leaves the π orbitals essentially unaltered. Indeed, our previous resonance Raman and NMR spectra on **1c**·HCl showed that the ground state is not very much perturbed.[5a] Detailed theoretical discussions of orbital structures are given in the accompanying paper.

Concluding Remarks

We have shown that the unusual red shift of absorption maxima in the visible region and the Soret band splitting observed for Schiff base porphyrins and chlorins upon protonation is due to the resonance effect of a strong electron-withdrawing group, not

(11) (a) O'Donnell, T. A. In "Comprehensive Inorganic Chemistry"; Trotman-Dickenson, A. F., Ed.; Pergamon Press: New York, 1973; Vol. 2, pp 1042–1049. (b) Emeleus, H. J. In "The Chemistry of Fluorine and Its Compounds"; Academic Press: New York, 1969; p 33. (c) The formation of $SBH^+HF_2^-$ is described by the following equilibria:

$$SB + HF \overset{K_1}{\rightleftharpoons} SBH^+ + F^-$$

$$HF + F^- \overset{K_2}{\rightleftharpoons} HF_2^-$$

In order for $SBH^+HF_2^-$ to form, K_2 should be greater than K_1, or on the basis of aqueous solution values, the pK_a of SBH^+ needs to be less than ca. 15. For SB·**4c**, a third equilibrium is introduced, due to the presence of the 7-OH moiety, namely:

$$7\text{-OH} + F^- \overset{K_3}{\rightleftharpoons} \text{O–H–F}^-$$

Due to the Coulombic attraction between SBH^+ and F^-, it does not seem unreasonable to expect that $K_3 > K_2$.

(12) Felton, R. H. In: "The Porphyrins"; Dolphin, D., Ed.; Academic Press: New York, 1978; Vol. V, pp 53.

delocalization of the positive charge onto the ring. We have further demonstrated that *the conversion of a carbonyl to a Schiff base peripheral group would subject the spectral properties of chlorin and porphyrin to a greater degree of environmental control than is otherwise possible.* In view of the large variations in the visible absorption maxima of photosynthetic chlorophylls, our result would certainly make a Schiff base chlorophyll an interesting model for reaction centers. Even more intriguing is the fact that there are large differences in oxidation potentials of P700 and P680. Titrations of P700 yield a midpoint potential ranging between +0.4 and +0.5 V vs. the normal hydrogen electrode (NHE) whereas the minimum potential needed to oxidize water to oxygen at physiological pH sets a lower limit of +0.8 V for P680,[13] which makes an electron-withdrawing system such as **4c** very attractive. Conceivably, the strong e-withdrawing group could also "pull away" spin density distributed at the reduced pyrrole ring in an oxidized chlorophyll cation radical resulting in a narrowing of the EPR signal line width. Further investigations, particularly EPR and electrochemical studies of Schiff base chlorophylls, are needed to verify the validity of these proposals.

Experimental Section

Visible spectra were recorded on a Cary 219 spectrophotometer interfaced to a Bascom-Turner recorder. Spectra shown in this paper were recalled directly from floppy diskettes. NMR spectra were obtained by using a Bruker WM-250 instrument. Elemental analyses were performed by Spang; C, H, and N analyses were within 0.5%. Cyclic voltammetry was performed by using a Bioanalytical Systems CV-1A unit or a Pine Instrument RDE-3 potentiostat in a specially constructed glass cell which contains two platinum spherical electrodes sealed through the cell wall. All measurements were carried out in THF containing 0.1 M tetrabutylammonium perchlorate at a scan rate of 100 mV/s.

Materials. CH_2Cl_2, CH_3CN, and triethylamine were freshly distilled from CaH_2 and tetrahydrofuran from lithium aluminum hydride before use. Pyrrolidine hydroperchlorate and hydrobromide were prepared by addition of the concentrated acid to pyrrolidine in THF till the solution was just acidic to wet pH paper. Water was azeotroped out with benzene on a rotary evaporator followed by three crystallizations from THF/ethyl acetate. Pyrrolidine hydrochloride was prepared by bubbling an ethereal solution of pyrrolidine with anhydrous HCl followed by crystallizations (3×) from THF/ethyl acetate. All other commercially obtained chemicals were used without further purification.

Nickel 2,6-Di-*n*-pentyl-4-vinyl-8-formyl-1,3,5,7-tetramethylporphine (1b). Chlorin **4a** (vide infra, 100 mg) in CH_2Cl (100 mL) was reduced by addition of sodium borohydride (50 mg) in methanol (2 mL) followed by quenching with dilute acetic acid after 5 min. The resultant diol porphyrin was dissolved in pyridine (100 mL) followed by addition of aqueous sodium periodate (5%, 30 mL), heated on a steam bath for 30 min, cooled, diluted with CH_2Cl_2, and extracted with 15% aqueous HCl. The crude product was purified by column chromatography using silica gel, crystallized from CH_2Cl_2–MeOH, and characterized by NMR and UV–vis spectroscopies. The yield of **1a** was 60 mg. Nickel insertion was accomplished by refluxing **1a** (60 mg) in CH_2Cl_2/MeOH with excess $Ni(OAc)_2$ for approximately 2 h followed by crystallization from CH_2Cl_2/MeOH. **1b**: yield 55 mg; NMR δ ($CDCl_3$) pentyl 0.89 (6 H, m), 1.95 (4 H, m), 3.53 (4 H, m); ring Me 3.16 (3 H, s), 3.20 (3 H, s), 3.37 (3 H, s), 3.42 (3 H, s); vinyl 6.09 (2 H, m), 7.94 (1 H, m); meso 8.97 (1 H, s), 9.13 (1 H, s), 9.29 (1 H, s), 9.96 (1 H, s); CHO 11.06 (1 H, s); λ_{max} (ϵ_{mM}) (CH_2Cl_2) 409 (114), 516 (5.9), 542 (6.9), 589 nm (21).

Nickel 6,7-Di-*n*-pentyl-1,4-diformyl-2,3,5,8-tetramethylporphine (2b) and Nickel 2,6-Di-*n*-pentyl-4,8-diformyl-1,3,5,7-tetramethylporphine (3b). The appropriate divinylporphyrin[9] (100 mg) dissolved in pyridine (100 mL) was added to a solution of osmium tetroxide (100 mg) in pyridine (10 mL) and stirred at room temperature for 1 h. To this was added an aqueous sodium sulfite solution (15%, 30 mL) followed by heating on a steam bath for 30 min and partition between CH_2Cl_2/H_2O. The porphyrin glycols were then oxidized with sodium periodate and purified as with **1a**. The yield for either porphyrin was ~80%. Nickel insertion was accomplished as with **1a** except that overnight reflux was necessary for completion. **2b**: NMR δ ($CDCl_3$) pentyl 1.01 (6 H, t), 1.58 (3 H, m), 2.00 (4 H, m), 3.52 (4 H, t); ring Me 2.52 (6 H, s), 3.52 (6 H, s); meso 8.82 (1 H, s), 9.39 (2 H, s), 10.54 (1 H, s); CHO 10.53 (2 H, s); λ_{max} (ϵ_{mM}) 423 (125) 535 (11.5), 578 nm (21). **3b**: NMR δ ($CDCl_3$) pentyl 0.92 (6 H, t), 1.55 (8 H, m), 1.90 (4 H, m), 3.5 (4 H, m); ring Me 3.10 (6 H, s), 3.42 (6 H, s); meso 8.83 (2 H, s), 9.76 (2 H, s); CHO 11.1 (2 H, s); λ_{max} (ϵ_{mM}) 412 (119), 509 (5.5), 607 nm (35).

2,6-Di-*n*-pentyl-4-vinyl-7-hydroxy-8-acroleinyl-1,3,5,7-tetramethylchlorin (4a) and 2,6-Di-*n*-pentyl-3,7-dihydroxy-4,8-diacroleinyl-1,3,5,7-tetramethylbacteriochlorin (5a). 2,6-Di-*n*-pentyl-4,8-divinyl-1,3,5,7-tetramethylporphine[9] (200 mg) in CH_2Cl_2 was photolyzed with aeration for 30 min in a water-cooled photolysis apparatus with a 250-W tungsten–halogen lamp. The reaction mixture was then concentrated and chromatographed on silica gel. CH_2Cl_2 elution afforded unreacted divinylporphyrin, followed by the monooxygen adduct then the trans diadduct. The cis diadduct was obtained by elution with 5% MeOH–CH_2Cl_2. Pure epimeric monoadduct and cis diadduct were crystallized from MeOH–CH_2Cl_2. Chlorin **1a** obtained (90 mg) in $CDCl_3$: NMR δ pentyl 0.89 (3 H, t), 0.96 (3 H, t), 1.5 (4 H, m), 1.98 (2 H, q), 2.12 (2 H, q), 3.7 (4 H, m); ring Me 1.60 (3 H, s), 3.22 (3 H, s), 3.45 (3 H, s), 3.51 (3 H, s); OH: 2.9 (1 H, b); vinyl 6.18 (2 H, m), 8.1 (1 H, m); =CHCHO 6.8 (1 H, d), 10.2 (1 H, d); meso-H 8.17 (1 H, s), 8.56 (1 H, s), 9.60 (1 H, s), 9.72 (1 H, s); NH −3.43 (1 H, s), −3.61 (1 H, s); λ_{max} (ϵ_{mM} in THF) 336 (24), 391 (80), 411 (91), 423 (89), 504 (6.1), 568 (18), 601 (7.9), 660 nm (46). *cis*-Bacteriochlorin **2a**: δ ($CDCl_3$) pentyl 0.88 (6 H, t), 1.5 (16 H, m), 1.93 (4 H, q), 3.76 (4 H, m); ring Me 1.63 (6 H, s), 3.14 (6 H, s); OH 5.84 (2 H, s); =CHCHO 7.14 (2 H, d), 10.58 (2 H, d); meso-H 8.30 (2 H, s), 8.55 (2 H, s); NH −4.41 (2 H, s); λ_{max} (ϵ_{mM} in THF) 350 (23), 419 (55), 443 (75), 581 (12), 659 (6.1), 692 (5.6), 729 nm (70). The trans isomer had identical spectral properties. Copper was inserted by standard procedures.[7]

Schiff Base Formation. (i) Schiff Bases 1c, 2c, and 3c. Nickel formylporphyrins **1b**, **2b**, and **3b** were refluxed in benzene containing excess *n*-butylamine for 3 h. Water produced was removed by allowing the condensate to filter through a silica gel pad prior to returning to the flask. Lypholyzation afforded pure **1c**, **2c**, and **3c**. The Schiff bases were each characterized by NMR and UV–visible spectroscopies. **1c**: NMR δ ($CDCl_3$) pentyl 0.94 (6 H, t), 1.50 (3 H, m), 2.09 (4 H, m), 3.71 (4 H, m); butyl 1.18 (3 H, t), 1.63 (2 H, m), 1.82 (2 H, m), 4.07 (2 H, t); ring Me 3.29 (3 H, s), 3.34 (3 H, s), 3.47 (3 H, s), 3.54 (3 H, s); vinyl 6.08 (2 H, m), 8.06 (1 H, m); meso 9.50 (3 H, m), 9.65 (1 H, s); CHN 10.64 (1 H, s); λ_{max} (ϵ_{mM}) 404 (149), 515 (4.6), 538 (5.5), 577 nm (16). **2c**: NMR δ ($CDCl_3$) pentyl 0.96 (6 H, t), 1.52 (8 H, m), 2.09 (4 H, m), 3.72 (4 H, t); butyl 1.20 (6 H, t), 1.65 (4 H, m), 1.83 (4 H, m), 4.07 (4 H, t); ring Me 3.34 (6 H, s), 3.42 (6 H, s); meso and CHN 9.38 (1 H, s), 9.42 (3 H, s), 10.58 (2 H, s). **3c**: NMR δ ($CDCl_3$) pentyl 0.96 (6 H, t), 1.50 (8 H, m), 2.08 (4 H, m), 3.73 (4 H, t); butyl 1.18 (3 H, t), 1.64 (2 H, m), 1.83 (2 H, m), 4.06 (2 H, t); ring Me 3.25 (6 H, s), 3.56 (6 H, s); meso 9.51 (2 H, s), 9.54 (2 H, s); CHN 10.68 (2 H, s); λ_{max} (ϵ_{mM}) 407 (162), 515 (7.2), 541 (8.7), 584 nm (29).

(ii) **Schiff Base 4c.** To **4b** (2 mg) in CH_2Cl_2 (3 mL) was added 5 drops of *n*-butylamine and the solution was allowed to stand for 15 min followed by evaporation under a stream of dry argon. The absorption spectrum was identical with that from (iii) in CH_2Cl_2 or THF.

(iii) **Schiff Base by the Spectrophotometric Method.** To a $\sim 10^{-5}$ M solution of **1b**, **2b**, **3b** (CH_2Cl_2), **4b**, or **5b** (THF) was added 1 drop of *n*-butylamine, and then 1 mL of air equilibrated over concentrated HCl was bubbled through the solution. Reactions were complete within 10 min. Isosbestic points: **1b** to **1c** (nm), 375, 409, 500, 582; **2b** to **2c**, none; **3b** and **3c**, none; **4b** to **4c** (nm), 395, 436, 500, 591, 612, 635; **5b** to **5c**, none. To **4b** ($\sim 10^{-5}$ M) in CH_2Cl_2 was added 2 drops of a solution containing 3 drops of *n*-butylamine in 5 mL of CH_2Cl_2 and a catalytic amount of HCl. Reaction required about 2 h for completion. Isosbestic points: 396, 445, 517, 647 nm.

Pyrrolidinium Salt (4d). (i) To 5 mg of **4b** in CH_2Cl_2 (5 mL) was added 1 equiv of pyrrolidine hydroperchlorate and 1 drop of trimethyl orthorformate and the solution was allowed to stand 48 h at room temperature, diluted with benzene, and lypholysed. The UV–vis spectrum was identical with that obtained below. (ii) To $\sim 10^{-5}$ M **4b** in CH_2Cl_2 or THF was added a couple of crystals of pyrrolidine·$HClO_4$ and the spectrum monitored. Isosbestic points (THF): **4b** to **4d**·ClO_4 383, 459, 538, 662 nm.

Malononitrile Adduct (4f). (i) To $\sim 10^{-5}$ M **4b** in THF was added 1 drop of malononitrile and 1 drop of triethylamine. Reaction was complete within 10 min. Isosbestic points: 385, 457, 564, 659 nm.

(ii) **4a** (7 mg) was dissolved in 30 mL of THF. To this solution 4 drops of malononitrile and 3 drops of triethylamine were added. This was refluxed 2 h followed by dilution with ether. The ether phase was extracted with 20% acetic acid (4×), washed with H_2O (2×) and brine (2×), dried over anhydrous Na_2SO_4, and evaporated in vacuo: yield, quantitative; NMR ($CDCl_3$) δ *n*-pentyl 0.89 (3 H, t), 1.07 (3 H, t), 1.3 (4 H, m), 1.6 (6 H, m), 2.3 (2 H, m), 3.7 (2 H, m), 4.0 (2 H, m); ring Me 1.27 (3 H, s), 3.44 (3 H, s), 3.58 (3 H, s), 3.68 (3 H, s); OH 6.7 (1

(13) (a) Govindjee, Ed. "Bioenergetics of Photosynthesis"; Academic Press: New York, 1978. (b) Bearden, A. J.; Malkin, R. *Q. Rev. Biophys.* **1975**, *7*, 131–177. (c) Evans, M. C.; Sihra, C. H.; Slibus, A. R. *Biochem. J.* **1977**, *162*, 75–85.

H, s); vinyl 6.26 (2 H, m), 6.18 (1 H, m); =CHCH=C(CN)$_2$ 6.84 (1 H, d), 7.67 (1 H, s); meso H 8.26 (1 H, s), 9.86 (2 H, s), 9.89 (1 H, s); NH -3.6 (1 H, s), -4.1 (1 H, s).

Ethyl Cyanoacetate Adduct (4e). This was prepared as in (i) for malononitrile. Reaction required about 10 h for completion. Isosbestic points: 380, 455, 535, 655 nm.

Pyrrolidine Hemiaminal. To $\sim 10^{-5}$ M **1b** in THF or CH_2Cl_2 was added 1 drop of pyrrolidine. Reaction was completed within 30 min. Isosbestic points (THF): 321, ~370, 423, 496, 578, 602, 628 nm.

Schiff Base Protonation/Deprotonation. (i) HF, HCl, HBr in CH_2Cl_2: To $\sim 10^{-5}$ M **1c** or **4c** in CH_2Cl_2 was bubbled air which had been equilibrated over the respective concentrated acid. (This was easily accomplished by withdrawing the air inside a bottle of acid with a small syringe and then passing the air into the cuvette.) The resultant SB·HCl spectra were identical as in (ii). BF_3OEt_2 was introduced to SB·HF by bubbling BF_3OEt_2-saturated air through the solution. (ii) To $\sim 10^{-5}$ M Schiff base in CH_2Cl_2, THF, or CH_3CN was added dropwise an anhydrous HCl-saturated CH_2Cl_2 solution. (iii) HI: To $\sim 10^{-5}$ M **1c** or **4c** in CH_2Cl_2 was injected a small amount of HI vapor prepared by adding concentrated sulfuric acid to KI. (iv) $HClO_4$: To $\sim 10^{-5}$ M Schiff base in CH_2Cl_2, THF, or CH_3CN was added dropwise a 70% $HClO_4$-saturated methylene chloride solution. (v) SBH^+ were returned to the original SB by bubbling triethylamine-saturated air through the acidified solution.

Borohydride Reduction. To $\sim 10^{-5}$ M **4b** in CH_2Cl_2 was added a couple of crystals of tetrabutylammonium borohydride and the UV-vis spectrum monitored. Isosbestic points: 321, 370, 423, 496, 578, 602, 628 nm. Addition of 2 drops of a 1:1:1 CH_3OH:TFA:H_2O solution yielded a typical copper porphyrin spectrum. Isosbestic points: 313, 345, 369, 409, 544, 557, 582 nm, λ_{max} (Cu porphyrin) 400, 528, 570 nm.

Acknowledgment. This work was supported in part by the NSF. We thank Professor G. T. Babcock and Dr. Pat Callahan for kindling our interest in Schiff base porphyrins and Professor G. Maggiora for communicating results prior to publication. C.K.C. is an Alfred P. Sloan Fellow, 1980-1984, and a recipient of a Camille and Henry Dreyfus Teacher-Scholar Grant, 1981-1985.

Registry No. 1a, 86146-16-9; **1b**, 84195-13-1; **1c**, 84195-14-2; **1c**·HF, 90413-37-9; **1c**·HCl, 90413-38-0; **1c**·HBr, 90413-39-1; **1c**·HI, 90413-40-4; **1c**·$HClO_4$, 90413-41-5; **1c**·HBF_4, 90413-42-6; **2a**, 90413-52-8; **2b**, 90413-26-6; **2c**, 90413-27-7; **3a**, 86146-17-0; **3b**, 90413-28-8; **3c**, 90413-29-9; **4a**, 90413-53-9; **4b**, 90413-30-2; **4c**, 90413-31-3; **4c**·HF, 90413-43-7; **4c**·HCl, 90413-44-8; **4c**·HBr, 90413-45-9; **4c**·HI, 90413-46-0; **4c**·$HClO_4$, 90413-47-1; **4c**·HBF_4, 90413-48-2; **4d**, 90413-32-4; **4d**·Cl^-, 90413-49-3; **4d**·Br^-, 90413-50-6; **4d**·ClO_4^-, 90413-51-7; **4e**, 90413-33-5; **4f**, 90413-34-6; **5a**, 90413-54-0; **5b**, 90413-35-7; **5c**, 90413-36-8; **5c**·$(CF_3COOH)_2$, 90432-15-8.

Spectral Properties of Protonated Schiff Base Porphyrins and Chlorins. INDO-CI Calculations and Resonance Raman Studies

Louise Karle Hanson,*[1b] C. K. Chang,*[1a] Brian Ward,[1a] Patricia M. Callahan,[1a,c] Gerald T. Babcock,*[1a] and John D. Head[1b,d]

Contribution from the Department of Chemistry, Michigan State University, East Lansing, Michigan 48824, and the Department of Applied Science, Brookhaven National Laboratory, Upton, New York 11973. *Received October 6, 1983*

Abstract: INDO-CI calculations successfully reproduce the striking changes in optical spectra that occur upon protonation of mono- and disubstituted porphyrin, chlorin, and bacteriochlorin Schiff base complexes. They ascribe the changes to Schiff base C=N π^* orbitals which drop in energy upon protonation and mix with and perturb the π^* orbitals of the macrocycle, a result consistent with resonance Raman data. The perturbation is predicted to affect not only transition energies and intensities but also dipole moment directions. The symmetry of the porphyrin and the substitution site of the chlorin are shown to play an important role, especially in governing whether the lowest energy transition will red shift or blue shift. Blue shifts are calculated for protonation of ketimine and enamine isomers of pyrochlorophyll *a* (PChl). Comparison with reported optical spectra suggests that PChl *a* Schiff base may undergo isomerization upon protonation. Resonance Raman data on CHO, CHNR, $CHNHR^+$, and pyrrolidine adducts of chlorin demonstrate the isolation of the peripheral C=O and C=N groups from the macrocycle π system, intramolecular hydrogen bonding, and selective enhancement of $\nu_{C=N}$ for those species with a split Soret band. $\nu_{C=N}$ is observed with 488.0-nm excitation into the lower-energy Soret and absent for 406.7-nm excitation into the higher-energy Soret, a result predicted by the calculations.

Photosynthesis in algae and green plants functions via two chlorophyll (Chl)-mediated systems which cooperatively reduce carbon dioxide (Photosystem I, PS I) and oxidize water (PS II).[2] Light is absorbed by antenna pigments (mostly Chl) which then funnel the excitation energy to special chlorophylls within the reaction centers, P700 in PS I and P680 in PS II. These pigments function as phototraps by virtue of their red-shifted absorption spectra relative to the antenna Chl. P700 and P680 are the primary electron donors for the light-driven reactions; the electron transfer takes place from their first excited singlet states.

Monomeric Chl *a* absorbs at 663 nm in CH_2Cl_2/THF[3] and P680 and P700 at 680 and 700 nm, respectively. The redox potentials of P700 and P680 are also modulated, P700 is ~0.3-0.4 V easier and P680 is ~0.1-0.2 V more difficult to oxidize than Chl *a* in CH_2Cl_2.[4] The red-shifted absorption spectra have, until recently, been attributed to dimers or higher-order aggregates of Chl *a*.[4] Because of inconsistencies between spectroscopic data for P680[4] and P700[5,6] and dimeric models, interest has currently

(1) (a) Michigan State University. (b) Brookhaven National Laboratory. (c) Current address: Department of Biochemistry, Molecular and Cell Biology, Northwestern University, Evanston, Illinois 60201. (d) Current address: Quantum Theory Project, University of Florida, Gainesville, Florida 32611.

(2) For recent general surveys of photosynthesis see: Barber, J., Ed. "Primary Processes of Photosynthesis," Elsevier: Amsterdam, 1977. Clayton, R. K. "Photosynthesis: Physical Mechanisms and Chemical Patterns," Cambridge University Press: New York, 1980. "Photosynthesis"; Govindjee, Ed.; Academic Press: New York, 1982; Vol. 1.

(3) Fajer, J.; Fujita, I.; Davis, M. S.; Forman, A.; Hanson, L. K.; Smith, K. M. *Adv. Chem. Ser.* **1982**, *No. 201*, 489-514.

(4) Davis, M. S.; Forman, A.; Fajer, J. *Proc. Natl. Acad. Sci. U.S.A.* **1979**, *76*, 4170-4.

(5) (a) Wasielewski, M. R.; Norris, J. R.; Crespi, H. L.; Harper, J. *J. Am. Chem. Soc.* **1981**, *103*, 7664-5. (b) Wasielewski, M. R.; Norris, J. R.; Shipman, L. L.; Lin, C. P.; Svec, W. A. *Proc. Natl. Acad. Sci. U.S.A.* **1981**, *78*, 2957-61.

0002-7863/84/1506-3950$01.50/0